Anisotropy and Orientation of the Microstructure in Viscous Emulsions During Shear Flow

ARTICLE *in* LANGMUIR · MARCH 1998

Impact Factor: 4.46 · DOI: 10.1021/la971046h

4 AUTHORS, INCLUDING:

Jan Vermant
ETH Zurich
162 PUBLICATIONS **4,669** CITATIONS
SEE PROFILE

J. Mewis
University of Leuven
120 PUBLICATIONS **3,852** CITATIONS
SEE PROFILE

Anisotropy and Orientation of the Microstructure in Viscous Emulsions during Shear Flow

J. Vermant, P. Van Puyvelde, P. Moldenaers, and J. Mewis

Department of Chemical Engineering, K. U. Leuven, de Croylaan 46, B-3001 Leuven (Heverlee), Belgium

G. G. Fuller*

Department of Chemical Engineering, Stanford University, Stanford, California 94305

Received September 18, 1997. In Final Form: January 7, 1998

Flow small-angle light scattering and linear conservative dichroism are used to follow, in situ and time resolved, the flow-induced changes of the microstructure in viscous emulsions such as immiscible polymer blends. A dilute system consisting of poly(butadiene) droplets dispersed in a poly(isobutene) matrix has been used as a model system. Contrary to earlier rheo-optical work on such materials, the structure has been probed in the plane formed by the flow and the velocity gradient directions. In this manner, shape anisotropy as well as the orientation angle can be monitored continuously for droplet sizes where microscopic observation becomes difficult or even impossible. During steady-state shear flow the size-dependent orientation of the droplets could be detected. It is shown that the various morphological stages caused by a sudden increase in shear rate can be identified and quantified: droplet deformation and rotation, fibril formation, and development of interfacial instabilities leading to breakup and reorientation of the resulting small droplets. These latter stages result in very characteristic light-scattering patterns. Values for anisotropy and orientation are derived from dichroism and light-scattering data and compared with theoretical results for the case of affine droplet deformation.

I. Introduction

Subjecting a mixture of immiscible viscous fluids or a polymer blend to flow can strongly affect the microstructure. When one phase is dispersed in the other, the flow will cause the inclusions to deform, break, and/or coalesce. Early work focused on direct microscopic observation of single droplets (see e.g. the reviews by Rallison[1] and Stone[2]). Since then, various techniques have been proposed to follow in situ the evolution of the microstructure in more *concentrated* and hence more realistic mixtures or blends. Rheological (e.g. refs 3−6), dielectrical,[7,8] and various scattering techniques[9] have been applied for this purpose. Recently, the use of linear conservative dichroism has been introduced as a tool to follow the evolution of microstructure under flow in real time.[10] Such measurements have been supplemented with qualitative observations of SALS patterns to identify the time scales for droplet deformation, fibril breakup, and coalescence. However, these observations were restricted to the velocity−vorticity (or 1−3) plane, as the opacity of the samples required a parallel plate geometry. In this manner the global anisotropy of the blend structure during flow could be studied, but no information concerning orientation was obtained. In the present work, because of a suitable choice of the model system, a Couette geometry could be used which enables one to observe the structural changes in the velocity-gradient (or 1−2) plane. Information about the microstructure can be derived from measurements of the dichroism as well as from SALS patterns. In this paper, combined information about the orientation angle and anisotropy of deformed droplets can be exploited to distinguish and characterize the various stages and changes in droplet morphology. Results on dilute blends can be used to evaluate existing predictions for single droplets or to explore possible extensions of the theories for example for viscoelastic fluids.

II. Experimental Section

A. Materials. The experiments are performed on a model polymer blend which has a droplet/matrix morphology and is liquid at room temperature. Emulsions containing 3% poly(butadiene) (PB, $M_w \sim 4500$ from Janssen Chemical) dispersed in poly(isobutene) (PIB, Parapol 950 from Exxon Chemical) are used. These polymers have been selected as model components because they are immiscible and have closely matched refractive indices ($n_{PB} = 1.520$ and $n_{PIB} = 1.499$). The latter is a requirement for the optical measurements, as the optical path length is quite substantial in a Couette geometry. The interfacial tension between the two polymers amounts to approximately 0.20 mN/m.[11] At 23 °C the zero shear viscosity of PIB is 30 Pa·s, whereas in the case of PB it is 8.1 Pa·s, resulting in a viscosity ratio of 0.27. For both neat PB and PIB the viscosity is independent of shear rate and no significant elasticity could be measured in the shear rate range under investigation. To obtain reproducible initial conditions, the blend has always been presheared at a shear rate of 1 s^{-1} for more than 1000 strain units.

B. Linear Conservative Dichroism. Linear dichroism refers to the anisotropy of the imaginary part of the refractive

* Corresponding author. E-mail: ggf@chemeng.stanford.edu.

(1) Rallison, J. M. *Annu. Rev. Fluid Mech.* **1984**, *16*, 45.
(2) Stone, H. A. *Annu. Rev. Fluid Mech.* **1994**, *26*, 65.
(3) Vinckier, I.; Moldenaers, P.; Mewis, J. *J. Rheol.* **1996**, *40*, 613.
(4) Vinckier, I.; Moldenaers, P.; Mewis, J. *J. Rheol.* **1997**, *47*, 705.
(5) Takahashi, Y.; Kurashima, N.; Noda, I.; Doi, M. *J. Rheol.* **1994**, *38*, 699.
(6) Friedrichn, C.; Gleinser, W.; Korat, E.; Maier, D, Weese, J. *J. Rheol.* **1995**, *36*, 1411.
(7) Boersma, A.; Wubbenhorst, M.; van Turnhout, J. *Macromolecules* **1997**, *30*, 2915.
(8) Tajiri, K.; Ohta, K.; Nagaya, T.; Orihara, H.; Ishibashi, Y.; Doi, M.; Inoue, A. *J. Rheol.* **1997**, *41*, 335.
(9) Søndergaard, K., Lyngaae-Jørgenson, J. *Rheo-physics of multiphase fluids*; Technomic Publishing Company: Lancaster, 1996.
(10) Yang, H.; Zhang, H.; Moldenaers, P.; Mewis, J. *Polymer*, in press.
(11) Van Puyvelde, P.; Yang, H.; Moldenaers, P.; Mewis, J. *J. Colloid Interface Sci.*, in press.

S0743-7463(97)01046-9 CCC: $15.00
Published on Web 03/04/1998

index.[12] By properly selecting the wavelength of the light source, anisotropy caused by scattering will dominate the contribution from absorption. As a result the so-called conservative dichroism is directly related to the anisotropy and orientation of the microstructure existing at a particular instant. This makes it an interesting observable to study flow-induced structures.

The instrument used here to measure linear dichroism, a Rheometrics Optical Analyzer (ROA), is based on a rotary polarization modulation principle, as suggested by Fuller and Mikkelsen.[13] It is a strain-controlled device. The optical train consists of a polarizer and a half-wave plate rotating at a frequency (ω) 2 kHz, which provides a modulation of the incoming light at a frequency of 8 kHz. For a dichroic sample, in the limit of small anisotropies, the intensity of the light transmitted by the sample is given by[12]

$$I = \frac{I_o}{2}[\cosh \delta'' - (\cos 2\theta \sinh \delta'') \cos 4\omega t - (\sin 2\theta \sinh \delta'') \sin 4\omega t] \quad (1)$$

with I_o the intensity of the incoming light, θ the orientation angle, and δ'' the extinction. The "DC" part of the transmitted light intensity ($I_o/2 \cosh \delta''$) is filtered out by using a low pass filter. Phase-sensitive detectors (lock-in amplifiers, Stanford Research Systems model 530) are used to determine the in-phase and out-of-phase components of the light intensity transmitted by the sample. From the measured values of I_{DC}, $I_{\cos 4\omega t}$ and $I_{\sin 4\omega t}$, the orientation angle θ and the magnitude of the dichroism ($\Delta n'' = \delta'' \lambda/(2\pi d)$, with d the thickness of the sample) can be determined simultaneously. The high modulation frequency makes it possible to study fast time-dependent phenomena. More details on this technique are given by Fuller.[12] A Couette cell is used here to probe the anisotropy in the flow-velocity gradient plane. The path length of the beam through the Couette flow cell is 2.44 cm. Some measurements have been performed using a parallel plate geometry, hence probing the flow−vorticity plane, in order to evaluate the non-axisymmetrical nature of the deformed drops.

C. Light Scattering. The light-scattering setup, used to measure the time-dependent SALS patterns, is described in more detail in ref 14. A Uniphase He−Ne laser provides a source of monochromatic light ($\lambda = 632.8$ nm). The light travels along the vorticity direction between two concentric cylinders, providing light-scattering patterns associated with the flow−velocity gradient plane. The path length of the beam through the flow cell is 1 cm. The scattered light is collected on a reflecting screen containing a pinhole which enables the light transmitted at zero scattering angle to pass through. The light scattered at nonzero angles generates an image on the screen which is then recorded from the top using a CCD camera placed at an angle relative to the incident beam. A simple linear transformation is performed on the digitized images to remove the geometric effect of viewing the scattering pattern at an angle.

The CCD camera is connected to a frame grabber (Data Translation DT2856) installed on a 80486-based host computer. This makes it possible to digitalize the images in real time. In this manner time-dependent phenomena can be followed. The gray level of the pixels is proportional to the intensity of the scattered light. The intensity profiles of the scattered light can thus be obtained as a function of the scattering vector ($|\mathbf{q}| = (4\pi/\lambda) \sin(\theta/2)$). To characterize the degree of anisotropy and the orientation of the scattering patterns, the second moment tensor is constructed from the measured light intensity on the 2-D CCD array. A measure of the degree of anisotropy ϵ may be obtained from the difference between the eigenvalues of this tensor:[15]

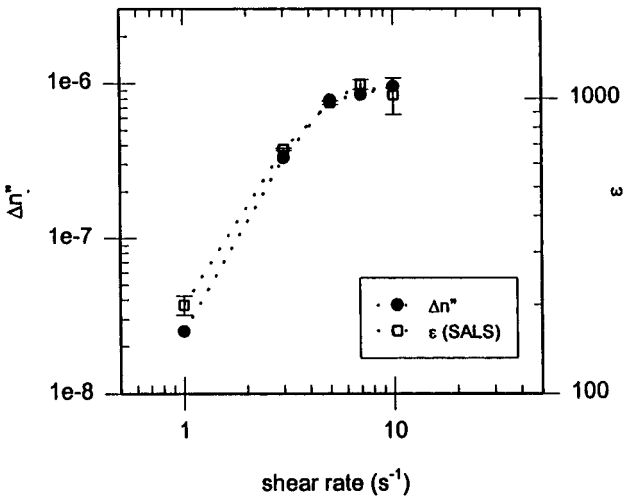

Figure 1. Dichroism $\Delta n''$ and anisotropy of the scattering patterns (ϵ) in the 1−2 plane as a function of shear rate.

$$\epsilon(\dot\gamma,t) = \{[(\int d\mathbf{q}\, q_x q_x I(q,\dot\gamma,t) - \int d\mathbf{q}\, q_y q_y I(q,\dot\gamma,t))^2 + 4(\int d\mathbf{q}\, q_x q_y I(q,\dot\gamma,t))^2]^{0.5}\}/\{\int d\mathbf{q}\, I(q,\dot\gamma,t)\} \quad (2)$$

Similarly, an orientation angle can be computed from

$$\tan(2\chi(\dot\gamma,t)) = \frac{2\int d\mathbf{q}\, q_x q_y I(q,\dot\gamma,t)}{\int d\mathbf{q}\, q_x q_x I(q,\dot\gamma,t) - \int d\mathbf{q}\, q_y q_y I(q,\dot\gamma,t)} \quad (3)$$

Due to the nature of the scattering process, the orientation angle χ of the SALS pattern will be perpendicular to the orientation angle θ of the scattering elements: $\theta(\dot\gamma,t) = \chi(\dot\gamma,t) - 90°$.

III. Results and Discussion

A. Steady-State Behavior. The steady-state dichroism is shown in Figure 1 as a function of shear rate. The dichroism in the velocity−gradient plane increases with shear rate but saturates at higher shear rates. This agrees with similar observations made in the velocity−vorticity plane by Yang et al.[10]

In the dilute systems under consideration, the dichroism is generally caused by changes in the shape, size, and orientation of the droplets. The size and shape of the inclusions is governed by the balance of the hydrodynamic and interfacial stresses. The ratio of these two competing stresses is expressed by the capillary number Ca:

$$\mathrm{Ca} = \frac{\eta_m \cdot \dot\gamma \cdot R}{\sigma} \quad (4)$$

where η_m is the matrix viscosity, $\dot\gamma$ is the shear rate, R is the radius of the inclusions, and σ is the interfacial tension. Increasing the shear rate will tend to increase Ca and therefore the deformation of the droplets. This effect is, however, partially counteracted by a reduction in R, resulting in a nonlinear growth of the anisotropy with shear rate. It should also be kept in mind that the sensitivity of the dichroism to the droplet anisotropy varies with the size of the droplets. The information derived from the SALS patterns during flow should be consistent with the dichroism data. To verify this, the evolution of the anisotropy with shear rate has been calculated according to eq 2 from the SALS patterns. These data are also shown in Figure 1. Although the absolute values cannot be compared at this stage, the similarity of the evolution of the two sets of data indicates that the

(12) Fuller, G. G. *Optical rheometry of complex fluids*, Oxford University Press: Oxford, 1995.
(13) Fuller, G. G.; Mikkelsen, K. J. *J. Rheol.* **1989**, *33*,761.
(14) Van Egmond, J.; Werner, D.; Fuller, G. G. *J. Chem. Phys.* **1992**, *96*, 7742.
(15) Johnson, S. J.; Salem, A. J.; Fuller, G. G. *J. Non-Newtonian Fluid Mech.* **1990**, *34*, 89.

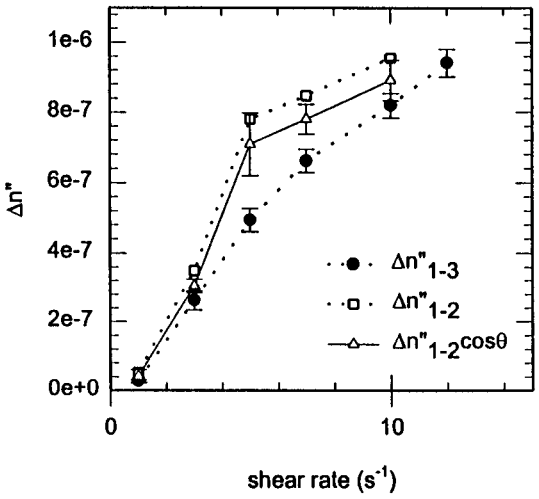

Figure 2. Comparison between dichroism measured in a Couette geometry and dichroism measured in a parallel plate geometry ($\Delta n''_{1-3}$).

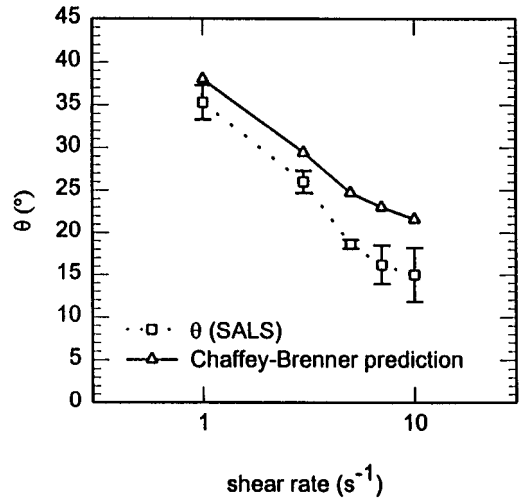

Figure 3. Orientation angle (θ) derived from the scattering patterns as a function of shear rate, compared to the predictions of the Chaffey−Brenner model.

dichroism is essentially determined by scattering at length scales that are probed in the SALS experiments.

Figure 2 compares the dichroism measured in the velocity−velocity gradient or 1−2 plane (Couette cell) with the dichroism measured in the velocity−vorticity or 1−3 plane (parallel plate geometry). It can be seen that, for the shear rates under investigation, the dichroism or anisotropy increases as a function of shear rate in both geometries. The dichroism is slightly larger in the 1−2 plane than in the 1−3 plane. In the latter, only a projection of the droplet is viewed, whereas, in the 1−2 plane, it is possible to probe their full anisotropy. The full line on Figure 2 represents the projection of the dichroism measured in the Couette cell on the 1−3 plane, taking into account the orientation angle of the droplets. Although the difference between the full curve and the measured dichroism in the 1−3 plane is small, the projected values seem to be systematically higher. The average ratio of the projection of the dichroism measured in the Couette cell over the dichroism in the 1−3 plane is 1.2. This could indicate a biaxial or non-axisymmetric nature of the deformed droplets. This has already been

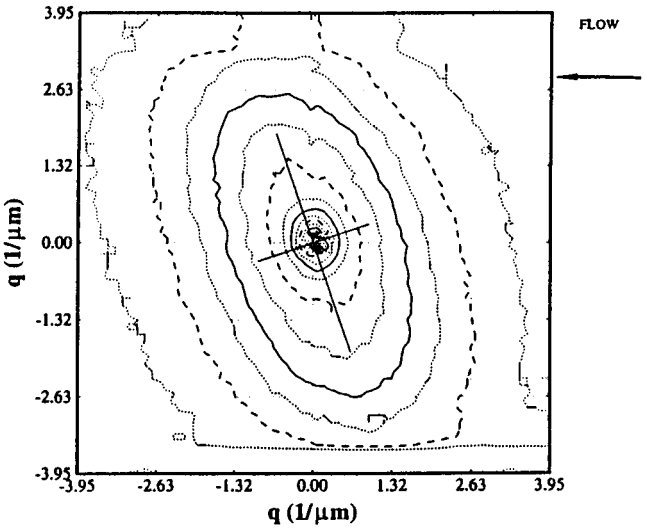

Figure 4. Contour plot of the SALS image as a function of the scattering vector for a steady-state SALS image at 5 s^{-1}.

observed for single droplets.[16,17] Levitt et al.[17] reported such an effect using strongly viscoelastic components and suggested that the biaxiality would depend on the difference in the second normal stress coefficient between the two phases. Interfacial tension of course always counteracts biaxiality. The samples under investigation are not very elastic, but on the other hand the interfacial tension is rather small, which could explain our observations. At any rate, it is interesting to note that dichroism measurements could be used to characterize biaxiality in systems that cannot be studied microscopically.

In addition to the anisotropy discussed above, the dichroism and SALS experiments provide information about the orientation angle of the inclusions. Using the SALS data and eq 3 provides the results displayed in Figure 3. The external shear forces will tend to orient the droplets in the flow direction whereas the interfacial tension and the viscous forces associated with the internal flow tend to shift the orientation toward 45°. The level of the extinction is too low in the present sample to provide accurate values for the orientation angle. However they could be used to detect qualitative trends, for example during fast changes (see further). The value of the steady-state orientation angle can also be calculated with a first-order approximation of the Chaffey−Brenner model,[18] which is known to give adequate predictions.[19] The angle as a function of capillary number is given by

$$\theta = \frac{\pi}{4} - \frac{(19p + 16)(2p + 3)}{80(p + 1)}\mathrm{Ca} \qquad (5)$$

where p is the viscosity ratio of the blend. The average radius of the droplets is obtained by analyzing the isotropic small-angle light-scattering patterns after relaxation of the steady shear flow.[10] As can be seen from Figure 3, the experimental data agrees quite well with the predictions of the Chaffey−Brenner theory. It is this orientation angle which has also been used to calculate the projected dichroism in Figure 2.

(16) Guido, S. Personal communication and BREU-Reports, Contract Number BREU2.CT92.0213.
(17) Levitt, L.; Macosko, C. W.; Pearson, S. D. *Polym. Eng. Sci.* **1996**, *36*, 1647.
(18) Chaffey, C. E.; Brenner, H. J. *J. Colloid Interface Sci.* **1967**, *24*, 258.
(19) Guido, S.; Villone, M. *Proc. XIIth Int. Congr. Rheol.* **1996**, 127.

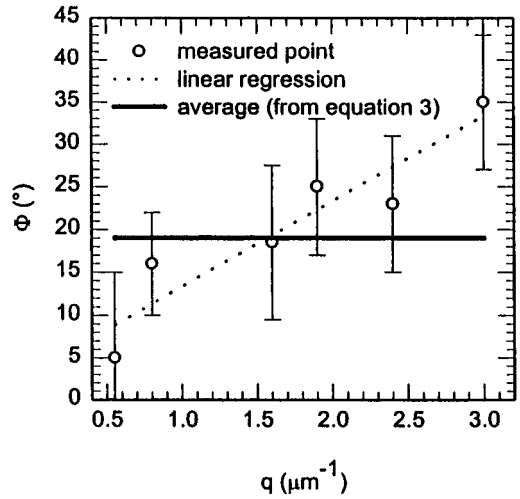

Figure 5. Orientation angle derived of the scattering patterns with respect to the velocity gradient direction (ϕ) as a function of the scattering vector for a shear rate of 5 s^{-1}.

Upon closer inspection of the detailed SALS patterns (Figure 4), it can be noted that the ellipses corresponding to different values of the intensity are not coaxial; hence, the orientation angle of the patterns varies with the scattering vector. Recently it has been observed that the aspect ratio of the isointensity curves varies with **q** for SALS patterns in the 1−3 plane.[21] In this plane the effect of orientation cannot be separated from that of shape. For small values of **q** in Figure 4 the patterns are more oriented toward the velocity gradient direction, meaning an orientation of the droplets toward the flow direction (zero angle). As **q** increases, the orientation angle increases as well. To quantify this effect, the orientation angle has been determined as a function of the scattering vector. The SALS patterns were sliced at a number of azimuthal angles, between O and 45° with respect to the velocity gradient direction. For given values of the scattering vector **q**, the angle at which the intensity reached its maximum was associated with the local orientation angle $\phi(q)$. The results are plotted in Figure 5 as a function of the scattering vector for the pattern presented in Figure 4. The angle is an increasing function of q. This agrees with the fact that the biggest drops, which scatter at the smallest angles, are oriented more toward the flow direction than the smaller drops. The same trend is predicted by eq 5. For the small drops, the orientation of the pattern is close to 45° with respect to the gradient direction, characteristic of an almost isotropic droplet oriented at 45° with respect to the flow direction. The results presented in Figure 5 clearly illustrate that there is indeed a distribution of droplet sizes. There is no straightforward manner to extract the size distribution from the present data: the inverse problem is ill-defined, and detailed information on the size distribution cannot be obtained without making some arbitrary assumptions.

B. Transient Flows. Time-resolved SALS and dichroism measurements were also used to study the deformation, breakup, and alignment of drops during transient flows. The blend was first presheared for a sufficiently long time at a shear rate of 1 s^{-1} to reach a steady-state morphology and then allowed to relax for 100 s. At that stage an isotropic microstructure consisting of spherical droplets was obtained. Subsequently, flow was started up again at a shear rate higher than 1 s^{-1}. In transient flows that correspond to capillary numbers greater than a critical capillary number, the drops will deform affinely

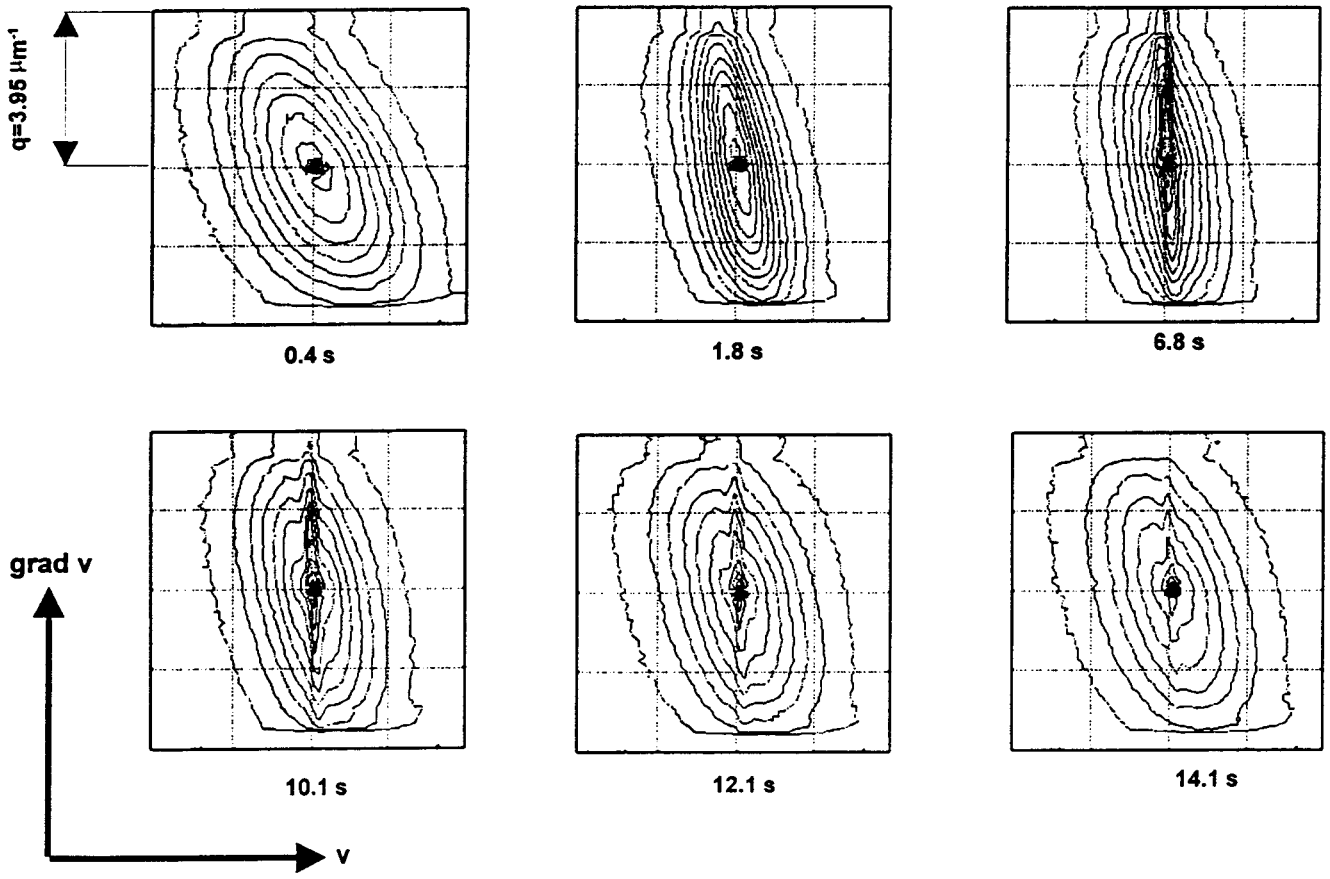

Figure 6. Contour plots of the SALS pattern during start-up of flow: preshear rate, 1 s^{-1}; shear rate, 7 s^{-1}.

into long slender bodies[22] that will eventually break up into small droplets. For viscosity ratios between 0.1 and 1 the critical capillary number is 0.5.[23] The shear rate corresponding to twice the critical capillary number is approximately 5 s^{-1}. An illustration of the SALS patterns resulting from such an experiment at a shear rate of 7 s^{-1} is given in Figure 6.

Initially, for example, during the first few seconds, the circular patterns deform and rotate gradually toward the velocity direction (Figure 6); the patterns resemble those obtained during steady-state shear flow. In transient flows the ellipses can continue to deform further, for example after 3.5 s. These strongly deformed patterns do not persist but develop into a remarkable scattering pattern consisting of a streak superimposed on an elliptical pattern which is tilted with respect to the streak (see for example after 12.1 s). Continued flow will lead to a reduction in intensity and eventually the disappearance of the streak to recover the ellipses characteristic of the steady-state behavior.

The evolution with strain of anisotropy and average orientation angle, calculated from the SALS patterns, is displayed in Figure 7 for various shear rates. At the lowest shear rate, well below twice the critical capillary number, only a small change in both the anisotropy and the orientation angle is observed. The situation becomes different at shear rates well above twice the critical capillary number, for example at 7 and 10 s^{-1}. After start-up, the anisotropy passes through a pronounced maximum (Figure 7a). At this point the orientation angle is nearing its minimum (Figure 7b). When the anisotropy starts to decrease, the orientation angle hardly changes for at least twenty strain units. The time resolution of the SALS experiments is limited; therefore, they were supplemented with dichroism measurements. The latter are represented in Figure 8. The qualitative agreement between the evolution of the anisotropy and the orientation is reasonable, again indicating that the dichroism is mainly caused by scattering on the length scales accessed in the SALS experiments.

The different stages in the evolution of the microstructure (for capillary numbers above twice the critical value) can be readily explained by the combined evolution of the anisotropy or dichroism and the orientation angle. Initially, the flow causes the droplets to deform, thus inducing an increasing anisotropy. The motion of the matrix fluid exerts a torque on the droplets which forces them to rotate toward the flow direction with increasing deformation. Under suitable conditions the droplets will continue to deform into long slender filaments, which will give rise to a streak in the scattering pattern. The initial deformation and orientation can be described by an affine motion, as the viscosity ratio is smaller than unity and the capillary number is larger than twice the critical value. The time-dependent orientation angle for an affine deformation is given by[22]

$$\theta = \frac{1}{2}\arctan\frac{2}{\gamma} \qquad (6)$$

The prediction of the time evolution of the orientation angle with this affine deformation theory is compared with the experimentally determined values in Figure 9. It can be seen that, when the applied shear rate is large enough, the affine deformation prediction agrees well with the experimental result up to the point where the orientation angle starts to increase again.

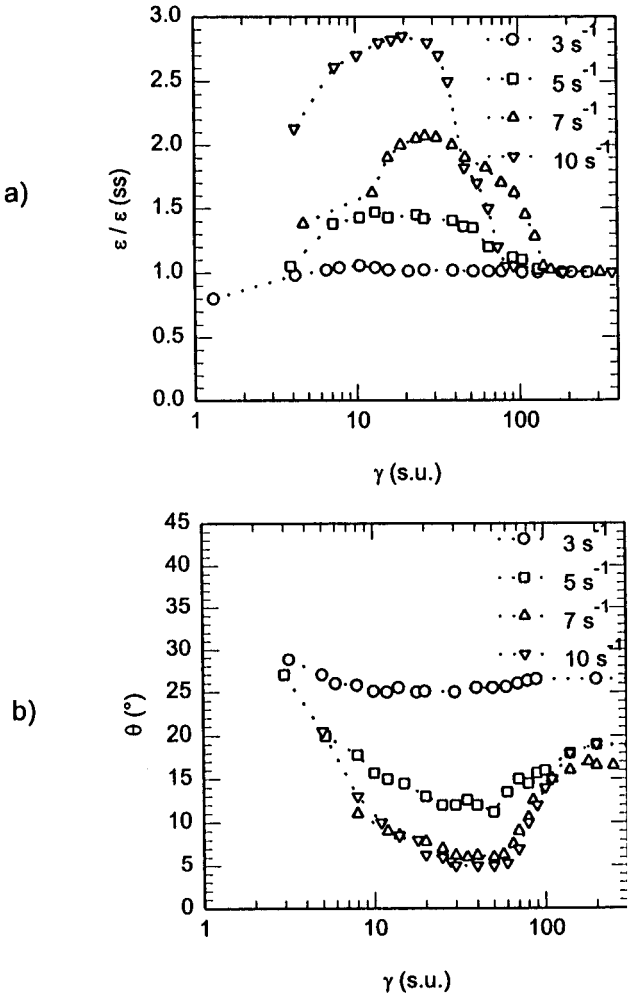

Figure 7. Evolution of the orientation angle (θ) and the anisotropy reduced by its steady-state value (ϵ/ϵ[ss]) of the SALS images observed during start-up of flow at various shear rates. Preshear rate, 1 s^{-1}.

The previous discussion deals only with the droplet deformation stage. Once stretched fibrils have been formed, interfacial instabilities will develop which will eventually lead to a disintegration of the filament. The growing disturbances on the interface will reduce the anisotropy and hence the dichroism. The decrease in anisotropy is also picked up by the measurement of normal forces in rheological experiments.[4] During this disintegration process, the fibrils remain oriented in the flow direction, as can be seen in Figures 7 and 8: the anisotropy decreases, but the orientation angle remains nearly constant. When the fibrils break up, small droplets are being formed. Because of the balance between hydrodynamic and interfacial forces, these droplets will reorient away from the flow direction toward the larger steady-state orientation angle corresponding to their smaller size. Hence the point at which the orientation angle starts to increase again can be identified with the point of fibril breakup.

In the region where the orientation angle increases again, the scattering patterns exhibit two features. Firstly, the deformed free droplets yield an elliptical pattern. Secondly, the aligned array of spheres resulting from the breakup of a fibril is responsible for the formation

(20) Cox, R. G. *J. Fluid Mech.* **1969**, *37*, 601.
(21) Rusu, D. Ph.D. thesis, Ecole des Mines de Paris, CEMEF, Sophia-Antipolis, 1997.
(22) Elemans, P. H. M.; Bos, H. L.; Janssen, J. M. H.; Meijer, H. E. H. *Chem. Eng. Sci.* **1993**, *48*, 267.
(23) Grace, H. P. *Chem. Eng. Commun.* **1982**, *14*, 225.

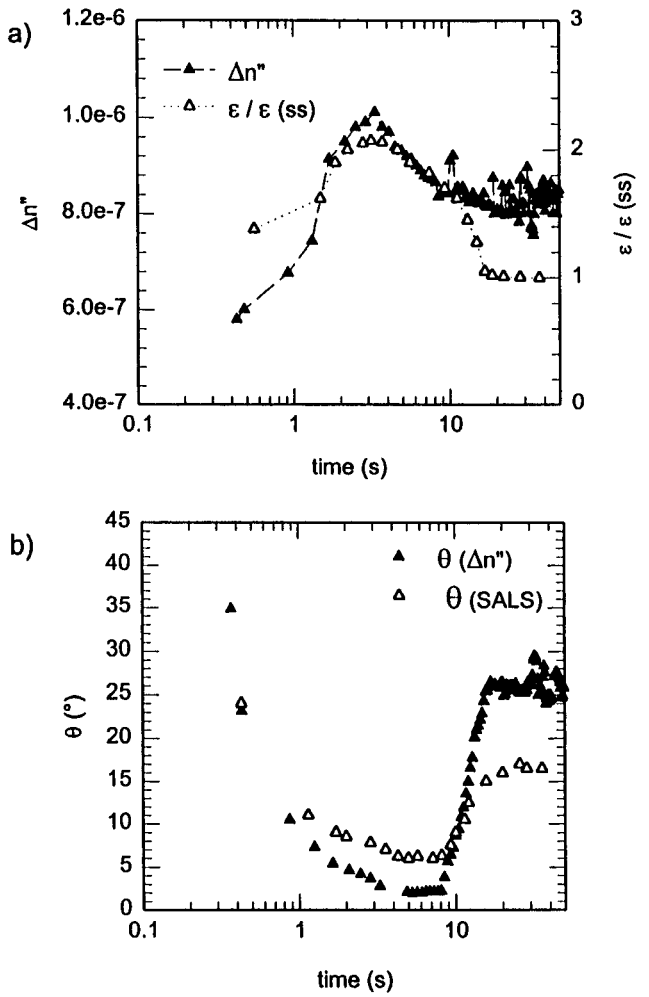

Figure 8. (a) Evolution of the dichroism ($\Delta n''$) as compared to the evolution of the reduced anisotropy (ϵ/ϵ[ss]) of the SALS images and (b) evolution of the orientation angles of the dichroism (θ) and of the SALS images (θ(SALS)), observed during start-up of flow at 7 s^{-1}. Preshear rate, 1 s^{-1}.

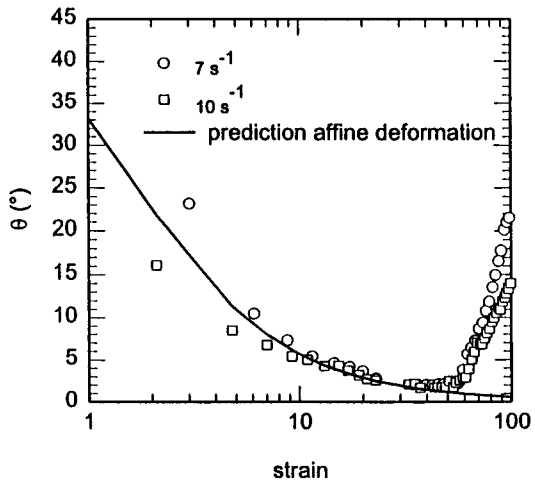

Figure 9. Comparison of the measured orientation angle of the dichroism with the predictions of an affine deformation.

of a streak perpendicular to the velocity direction. Because of interactions between droplets during flow, the linear ordering of the droplets is disturbed and the streak disappears, evolving gradually toward the steady-state elliptical scattering pattern.

The combined use of orientation angle and dichroism clearly identifies the time scale for breakup of the fibril. The maximum in dichroism or ϵ is indicative of the moment at which interfacial instabilities start to develop. The point where the orientation angle starts to turn away from the flow direction signals the breakup of the fibril. Hence the onset of instabilities and the breakup can be clearly separated.

The mechanism responsible for filament breakup in the experiment discussed above cannot be deduced unambiguously from the SALS images. Three different mechanisms are possible: tip streaming, end-pinching, and breakup through capillary (Rayleigh) instabilities. Tip streaming can be excluded, as it only seems to occur for low-viscosity ratios and for systems where surfactants are present.[24] Rayleigh instabilities are expected to develop for strongly stretched fibrils. They have indeed been observed during extensional flows by Mikami et al.[25] and Janssen et al.[26] In simple shear flows, the situation is less clear, as the shearing motion affects the upper and lower surfaces of the fibril in different ways. However, both Elemans et al.[22] and Rusu[21] report having observed Rayleigh instabilities during simple shear flow. The breakup times deduced from our rheo-optical experiments compare quite well with the values by Elemans et al., pointing possibly toward breakup by Rayleigh instabilities. However, if breakup by Rayleigh instabilities was the only mechanism present, diffraction peaks related to the wavelength of the disturbance would be visible in the scattering pattern.[27] These were not observed in the present case.

IV. Conclusions

Using flow-SALS and/or linear conservative dichroism, the anisotropy and orientation angle of the inclusions can be monitored, in situ and in real time, in two-phase liquid mixtures in flow conditions where microscopic observations become impractical or impossible. Not only the steady-state flow conditions can be probed by these rheo-optical techniques but also transient phenomena. In steady-state shear flow the SALS patterns reflect the distribution of droplet sizes, but the average orientation angle follows, at least qualitatively, the predictions derived for single droplets in Newtonian fluids. During transient flows quite detailed information about the morphological changes can be derived. This includes the time evolution of the orientation angle, the deformation of the droplet into fibrils, and the development of Rayleigh instabilities followed by fibril breakup. The affine nature of the deformation can be established, and the time scales for the different stages are obtained quantitatively. The rheo-optical techniques presented here are considered particularly useful in the case of immiscible polymer blends in order to study the effect of material properties, such as the viscoelasticity of the polymers, on the flow-induced morphology. For such phenomena neither a full theory nor systematic experiments are available at this moment.

Acknowledgment. One of us (J.V.) gratefully acknowledges support by Elf Aquitaine through a postdoctoral scholarship coordinated by Dr. B. Ernst (Elf Atochem) and NATO Grant 920239. G.G.F. acknowledges partial support from the NSF Polymer Program under Grant DMR-9522642. I. Vinckier and H. Yang (K. U. Leuven) are thanked for stimulating discussions.

LA971046H

(24) de Bruijn, R. A. *Chem. Eng. Sci.* **1993**, *48*, 277.
(25) Mikami, T.; Cox, R. G.; Mason, S. G. *Int. J. Multiphase Flow* **1975**, *2*, 113.
(26) Janssen, J. M. H.; Meijer, H. E. H. *J. Rheol.* **1993**, *37*, 597.
(27) Mewis, J.; Yang, H.; Van Puyvelde, P.; Moldenaers, P.; Walker, L. *Chem. Eng. Sci.*, in press.